Calculations of the electronic structure and superconducting properties of $BaPb_{1-x}Sb_xO_3$

J. P. Julien
Laboratoire d'Etudes des Propriétés Electroniques des Solides, Centre de la Recherche Scientifique, 25 avenue des Martyrs, Boîte Postale 166, 38042 Grenoble, France

D. A. Papaconstantopoulos
Complex Systems Theory Branch, Naval Research Laboratory, Washington, D.C. 20375-5000

F. Cyrot-Lackmann and A. Pasturel
Laboratoire d'Etudes des Propriétés Electroniques des Solides, Centre de la Recherche Scientifique, 25 avenue des Martyrs, Boîte Postale 166, 38042 Grenoble, France
(Received 23 July 1990; revised manuscript received 28 September 1990)

We have performed a band-structure calculation of the cubic perovskite compound $BaSbO_3$ by the augmented-plane-wave method. Using these results we have constructed an accurate tight-binding Hamiltonian which we used to calculate the density of states of the alloy $BaPb_{0.75}Sb_{0.25}O_3$ by the coherent-potential approximation. We have also calculated the electron-phonon coupling and found that such coupling can explain the low transition temperature T_c of this alloy system and the higher T_c for the Bi-doped alloy. A prediction is made for a much higher transition temperature for Sb- or Bi-rich alloys.

I. INTRODUCTION

Before the discovery of Bednorz and Müller[1] on copper-based compounds, some oxides were already known to be superconducting. Among them, the most interesting behavior was observed in the perovskite-type alloy $BaPb_{0.7}Bi_{0.3}O_3$, which is characterized by a superconducting transition around 12 K,[2] and a low density of states (DOS) at the Fermi level.[3] More recently, the cubic perovskite compound $Ba_{0.6}K_{0.4}BiO_3$ has been found to be superconducting at 30 K.[4] In addition to the copper-based oxides, these materials also present a great interest for several reasons. First the superconductivity occurs in a three-dimensional arrangement. Second, the semiconducting monoclinic perovskite compound $BaBiO_3$ exhibits a charge-density wave (CDW) due to the charge disproportionation of the bismuth atom in Bi^{3+} and Bi^{5+}.[5] This disproportionation could be considered as the electronic equivalent of antiferromagnetism in the copper compounds. The substitution of Ba by K suppresses the CDW and leads to the cubic perovskite structure for the $Ba_{0.6}K_{0.4}BiO_3$ superconducting alloy.

Very recently, Cava *et al.*[6] have tried a new candidate for superconductivity in the system $BaPb_{0.75}Sb_{0.25}O_3$ in which they have found a very low critical temperature T_c of 3.5 K. This value is surprisingly low in view of the similarities with the compound $BaPb_{0.75}Bi_{0.25}O_3$ that has a T_c of 12 K. The Sb atom ($5s^25p^3$) is electronically very similar to the Bi atom ($6s^26p^3$); so assuming that the only difference in an electron-phonon coupling comes through the mass dependence, the substitution of Bi by Sb would lead to a higher T_c, in contradiction to the observed result. We will show in this paper that the effect of the Sb or Bi mass is overcome by changes in the electron-ion matrix elements.

In this paper, which is a continuation of our work on $BaPbO_3$, $BaBiO_3$, and $KBiO_3$ (Ref. 7), we present a study of the electronic structure of the compound $BaSbO_3$ in the cubic perovskite structure using self-consistent augmented plane wave (APW) band calculations, and use these results to evaluate the electron-phonon interaction parameter. We have also performed a fit of the APW band structure to a tight-binding Hamiltonian with an orthogonal basis giving a set of Slater-Koster parameters. These parameters, and those obtained for $BaPbO_3$,[7] are used to study the effect of disorder for the alloys $BaPb_{1-x}Sb_xO_3$ by the coherent-potential approximation (CPA).

II. DESCRIPTION OF THE COMPUTATIONAL METHODS

We have performed a self-consistent and scalar-relativistic APW calculation for cubic-perovskite-structure $BaSbO_3$ in the muffin-tin approximation. The lattice constant of the pure compound has been chosen to be equal to 8.0302 a.u. which is the observed value for the alloy $BaPb_{0.5}Sb_{0.5}O_3$.[6]

The scalar-relativistic APW calculation includes the mass-velocity and Darwin terms in the Hamiltonian but neglects the spin-orbit coupling. The levels that were treated as bands are Ba($5p,6s$), Sb($5s,5p$), and O($2s2p$). The inner levels were not frozen but recalculated at each iteration by an atomic code that included the spin-orbit coupling. The exchange-correlation potential was treated in the local-density approximation using the Hedin-Lundqvist formula. To achieve self-consistency, we made the calculation on a 10-**k** point mesh in $\frac{1}{48}$th of the Brillouin zone (BZ). After 14 iterations, the Fermi level was

converged within 3 mRy. Then, the final potential was used to obtain the eigenvalues for 35 **k** points in $\frac{1}{48}$th of the BZ. These eigenvalues were interpolated to a grid of 165 **k** points using the symmetrized Fourier-series method of Boyer[8] and then the densities of states (DOS) were obtained by the tetrahedron method.[9] The values $N_1(E_F)$ of the DOS at the Fermi level, E_F, together with the scattering phase shifts were used in the rigid-muffin-tin approximation[10] (RMTA) to calculate the McMillan-Hopfield parameter η.

The APW eigenvalues have been used to perform a Slater-Koster (SK) fit of the band structure retaining the Ba s, Sb s,p, and O p orbitals. The resulting 14×14 orthogonal tight-binding Hamiltonian involving 17 two-center parameters has been determined by a least-squares procedure with a fitting error of 13 mRy. The (SK) parameters that we will also use in the CPA calculations are given in Table I.

Finally, using the tight-binding Hamiltonian where the on-site energies are replaced by energy-dependent self-energies Σ, we applied the CPA.[11] In the CPA one assumes zero scattering on average, according to the following condition that determines the self-energies:

$$x(\varepsilon_A-\Sigma)[1-(\varepsilon_A-\Sigma)G]^{-1} +(1-x)(\varepsilon_B-\Sigma)[1-(\varepsilon_B-\Sigma)G]^{-1}=0 . \quad (1)$$

x represents the concentration of A component and $\varepsilon_A,\varepsilon_B$ the on-site energies for the A and B components. G is the effective Green function, obtained by integration over the BZ by the formula

$$G=\int_{\mathrm{BZ}}\frac{dk}{z-\bar{H}(k)} , \quad (2)$$

where z is the complex energy and $\bar{H}(k)$ is an effective Hamiltonian obtained from the unperturbed one by replacing ε_A or ε_B by Σ. The effect of the off-diagonal disorder has been taken into account by a geometrical average of the hopping parameters of the pure compounds. It should be noted that the substitution of Pb by Sb involves s and p orbitals. Thus we need to determine two self-energies Σ_s and Σ_p by solving two equations of the form (1).

TABLE I. Slater-Koster parameters (in units of Ry).

	$BaSbO_3$	$BaPbO_3$
On-site energies		
Ba s	0.8223	0.6832
Sb s	0.3816	0.4960
Sb p	1.4328	1.0857
O p	0.3293	0.3498
First-neighbor hopping integrals		
Ba-Ba ($ss\sigma$)	−0.0049	−0.0325
Sb-Sb ($ss\sigma$)	−0.0104	−0.0046
Sb-Sb ($sp\sigma$)	0.0288	0.0020
Sb-Sb ($pp\sigma$)	−0.0456	−0.0973
Sb-Sb ($pp\pi$)	0.0207	0.0322
O-O ($pp\sigma$)	0.0368	0.0510
O-O ($pp\pi$)	0.0056	0.0159
Ba-Sb ($ss\sigma$)	−0.0132	−0.0088
Ba-Sb ($sp\sigma$)	−0.0250	−0.0242
Ba-O ($sp\sigma$)	0.0609	0.0500
Sb-O ($sp\sigma$)	−0.1496	−0.1463
Sb-O ($pp\sigma$)	0.2052	0.1361
Sb-O ($pp\pi$)	0.0121	0.0828

III. BAND-STRUCTURE RESULTS

A. APW results

The APW band structure of $BaSbO_3$ is shown in Fig. 1. There are mainly three groups of bands. The lowest states, around −0.8 Ry, are due to the O $2s$ levels. A narrow band located at −0.2 Ry corresponds to the $5p$ levels of Ba. Then the wide band group between −0.1 Ry and 0.8 Ry comes from the mixing of the Sb $5s$ and $5p$ levels with the O $2p$ levels. The states contributing to the Fermi level have a dominant O $2p$ character and the Sb $5s$ and $5p$ characters are smaller as can be seen from a partial wave analysis of the APW densities of states given in Table II.

This band structure should be compared to that of $BaBiO_3$ (shown in Fig. 2 of Ref. 7) which is a compound with an equal number of valence electrons. We note near E_F a striking similarity between $BaSbO_3$ and $BaBiO_3$, characterized by the feature that the top band crossing E_F is nearly half-filled. The lower bands have a pronounced difference in the position of the band that originates at Γ_1, which has predominantly Sb or Bi s-like character. This band while in $BaSbO_3$ lies in between the O p–like states, in $BaBiO_3$ is much lower and, at the high-symmetry point R, mixes with the narrow Ba $5p$ levels. It is interesting to note that the positioning of this Sb (or Bi) band with respect to the O and Ba bands is more similar to that of $BaPbO_3$ (shown in Fig. 1 of Ref. 7).

The density of states (DOS) presented in Fig. 2 shows a fairly low value at E_F and a region of high density starting just below 0.2 Ry and ending at about 0.4 Ry. The angular-momentum decomposition of the DOS demonstrates that the O p component is by far the strongest. The reader should note in Fig. 2 that the Ba s, Sb s, and Sb p components are given on a different scale than the total and O p DOS. Therefore, even at E_F the O p state density is the largest. This can be seen from Table II where one finds that n_p of the oxygen atoms is approximately a factor of 2 larger than the n_s of Sb.

B. Slater-Koster results

As we describe in Sec. II we performed a Slater-Koster (SK) fit to the APW energy bands. The SK parameters are given in Table I and the resulting densities of states

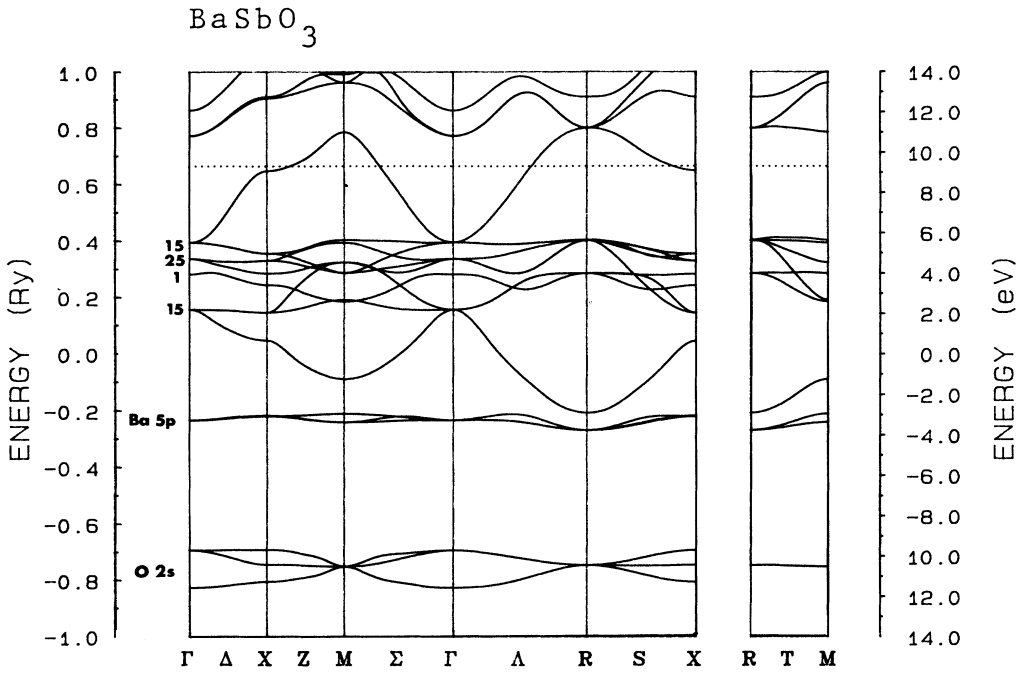

FIG. 1. Energy bands of $BaSbO_3$.

TABLE II. Fermi level values of DOS, velocity, plasmon energy, muffin-tin values of the l components of the DOS, the ratio $R_l = n_l / N_l$, phase shifts δ_l and electron-phonon parameter η.

	$BaSbO_3$		
E_F (Ry)	0.6660		
$N(E_F)$ (states/Ry spin)	5.1371		
$V(E_F)$ (cm/s)	0.78×10^8		
$\Omega(E_F)$ (eV)	3.96		
	Ba	Sb	O_3
n_s (states/Ry spin)	0.0003	1.1952	0.2457
n_p (states/Ry spin)	0.0046	0.2153	2.4526
n_d (states/Ry spin)	0.0063	0.0415	0.1164
n_f (states/Ry spin)	0.0168	0.0013	0.0092
R_s	0.0010	6.6869	3.1302
R_p	0.0092	0.2475	2.2501
R_d	0.0028	0.7690	2.3765
R_f	0.0507	0.1866	3.7266
$\sin^2(\delta_s-\delta_p)$	0.4343	0.0475	0.2078
$\sin^2(\delta_p-\delta_d)$	0.8070	0.3413	0.5829
$\sin^2(\delta_d-\delta_f)$	0.0109	0.0002	0.0001
η_{sp} (eV/Å^2)	0.0	0.1003	0.6227
η_{pd} (eV/Å^2)	0.0001	0.1658	2.6525
η_{df} (eV/Å^2)	0.0	0.0002	0.0017
η_{tot} (eV/Å^2)	0.0001	0.2663	3.2769

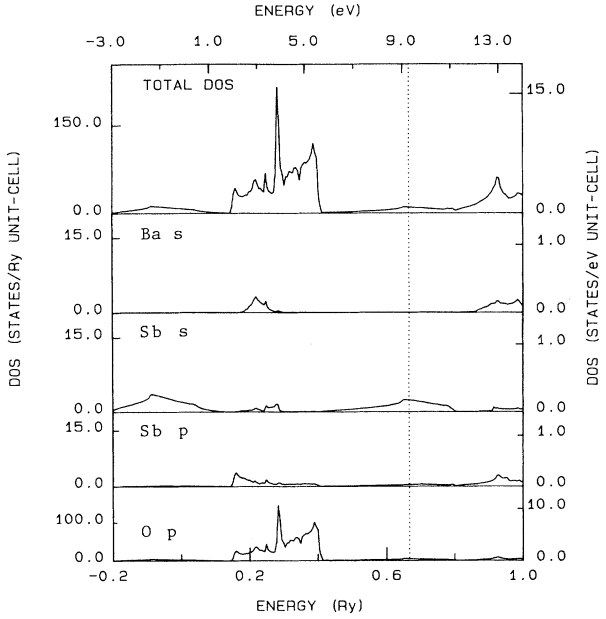

FIG. 2. APW densities of states for $BaSbO_3$. Note the variable scale for the different angular-momentum components.

(DOS) are presented in Fig. 3. Comparison of the on-site SK parameters given here with those for $BaPbO_3$ and $BaBiO_3$ that appear in Table III of Ref. 7 reveals that while the O p parameters are of about equal strength for all three compounds, the s and p on site energies of Sb are close to the average values of Pb and Bi. This is consistent with the energy band comparison made in Sec. III A where we point out common features of the $BaSbO_3$ bands to those of both $BaPbO_3$ and $BaBiO_3$.

Comparison of Fig. 3, showing the SK DOS, to the APW DOS of Fig. 2 results in excellent agreement near E_F and a fairly good agreement in the entire spectrum. This demonstrates the good quality of the SK fit and becomes important for the CPA calculations discussed below.

C. CPA results

We have studied the $BaPb_{1-x}Sb_xO_3$ alloys in the range x from 0.2 to 0.3 which correspond to the critical concentration where superconductivity occurs. Figure 4 shows the DOS for x equal to 0.25. The structure of the DOS is very similar to those of $BaPbO_3$ and $BaSbO_3$ with only some minor differences in the shape of the DOS, and of course in the position of E_F. We notice the general trend to lower the DOS at the Fermi level when one decreases the doping in Sb as E_F moves in a region of a continuously decreasing DOS. This tendency is also suggested by a rigid-band argument when one analyzes the DOS of the pure $BaPbO_3$ (after Ref. 7).

D. Charge transfer

We have integrated our APW DOS for each atom and found that in $BaSbO_3$ the electronic charges are distributed as follows: 0.19+ for Ba, 3.45+ for Sb, and 0.88− per O atom. We consider the APW results for charge transfer as only indicative of the direction of the charge flow. The reason is that the APW results are muffin-tin

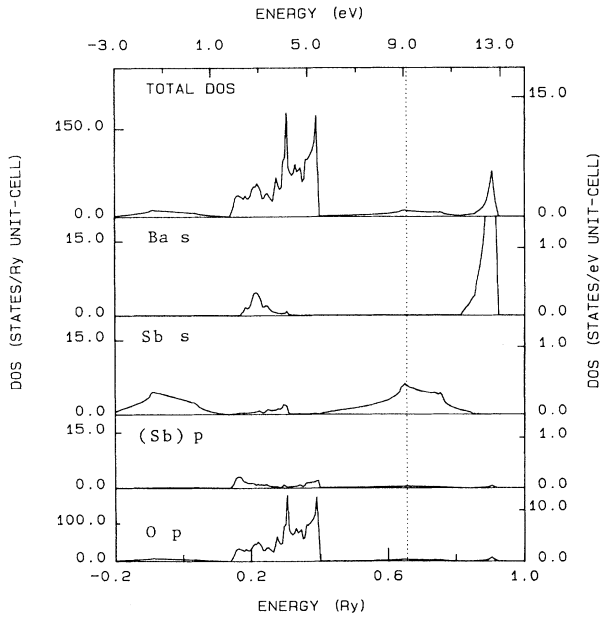

FIG. 3. Slater-Koster densities of states for $BaSbO_3$. Note the variable scale for the different angular-momentum components.

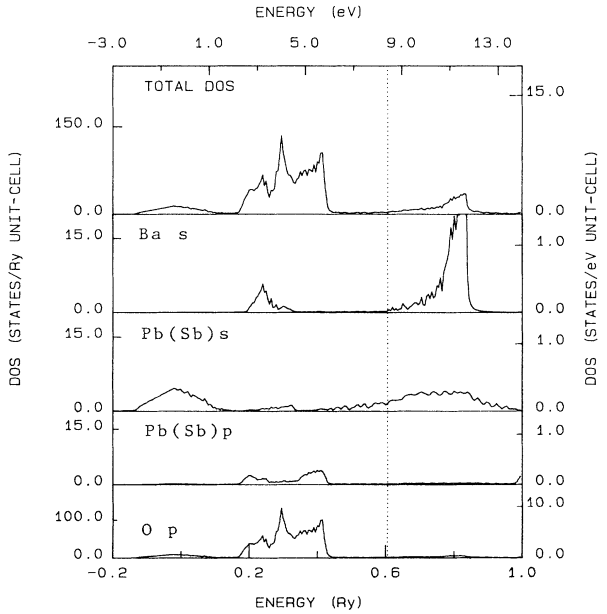

FIG. 4. CPA densities of states for $BaPb_{0.75}Sb_{0.25}O_3$. Note the variable scale for the different angular-momentum components.

radius dependent and since we have used for the Ba sphere a radius that is almost double that of Sb and O (see Ref. 7) the charge flow from Ba to O is underestimated. A better way to evaluate charge transfer in this compound is to integrate our SK DOS, which do not have the muffin-tin-sphere constraint. This calculation gives the following charge distribution: 1.76+ for Ba, 3.28+ for Sb, and 1.68− per O atom. We have also performed the same analysis with the CPA DOS at $x=0.25$ and find the following electron-charge distribution: 1.69+ for Ba, 2.80+ for Pb (Sb), and 1.50− per O atom. It is, therefore, clear that in the formation of this compound, charge transfer occurs from both Sb and Ba towards O.

IV. THE ELECTRON-PHONON INTERACTION

We have used the rigid-muffin-tin approximation of Gaspari and Gyorffy[10] to calculate the electronic part of the electron-phonon interaction, the so-called McMillan-Hopfield parameter, given by the expression

$$\eta_a=\frac{E_F}{\pi^2 N(E_F)}\sum_l 2(l+1)\sin^2(\delta_{l+1}^a-\delta_l^a)\frac{N_l^a N_{l+1}^a}{N_l^{(1)a}N_{l+1}^{(1)a}} . \tag{3}$$

In this expression the δ_l^a are the scattering phase shifts at E_F for atom α and angular momentum l. $N_l^{(1)a}$ are the single-scatterer densities of states defined in Ref. 10 and N_l^a are the site angular-momentum densities of states at E_F. The quantities that enter Eq. (3) as well as the results are summarized in Table II.

It is interesting to note from Table II that the strongest components of $N(E_F)$ are the O p-like and the Sb s-like. The resulting η values show that O is by far the biggest contributor and the dominant term is the p-d scattering of O. The latter is reminiscent of the situation in transition metals where the d-f scattering dominates. This has been understood in terms of d wave function tails appearing as f wave functions in a neighboring atom. It seems that we have an analogous situation here with the p wave functions.

Since our CPA results support rigid-band behavior in these systems we have used our APW results for $BaSbO_3$ and also for $BaBiO_3$, and applied Eq. (3) to calculate the η values as a function of number of electrons, thus simulating the $BaPb_{1-x}Sb_xO_3$ and $BaPb_{1-x}Bi_xO_3$ alloys. The results are displayed in Fig. 5 which shows that η_{Sb} and η_{Bi} are small and slowly varying with concentration x. On the other hand, η_O is much larger for both alloys and rapidly increases with x. A comparison of the η values of $BaPb_{1-x}Sb_xO_3$ to those of $BaPb_{1-x}Bi_xO_3$ shows that $\eta_{Bi}>\eta_{Sb}$ for all x, and for large x η_O is strongest in the Sb alloy while for small x η_O is strongest for the Bi alloy. Therefore, for $x=0.25$ these calculations clearly indicate a stronger electron-phonon interaction in $BaPb_{0.75}Bi_{0.25}O_3$ than in $BaPb_{0.75}Sb_{0.25}O_3$. Figure 5 also suggests that if a stable alloy can be made at high Sb or Bi concentrations, it could have a much higher superconducting temperature T_c. To estimate the value of T_c we have employed the McMillan equation with

$$\mu^*=0.1,\quad \lambda=\frac{1}{\langle\omega^2\rangle}\sum_\alpha\frac{\eta_\alpha}{M_\alpha}$$

and for a range of average phonon frequencies 200 K $<\omega<$ 400 K. The results are presented in Fig. 6 where

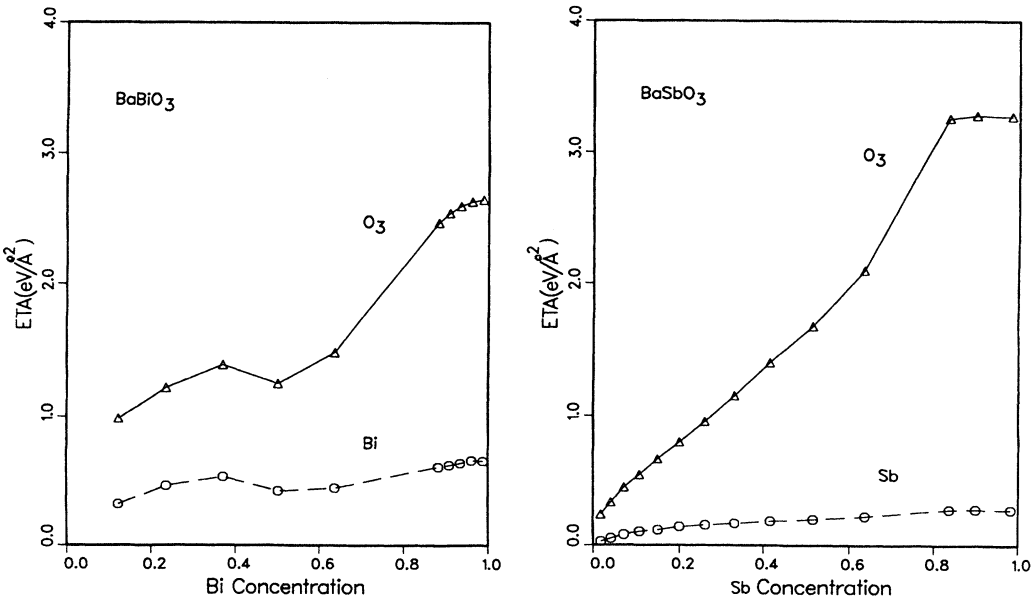

FIG. 5. Rigid-band variation of the η parameter in $BaBiO_3$ as a function of Bi concentration (left panel) and of $BaSbO_3$ as a function of Sb concentration (right panel).

T_c is plotted versus $\langle\omega\rangle$ (and λ) for the values of η given in Table II corresponding to $BaSbO_3$ and also for the η's that are found for $BaPb_{0.75}Sb_{0.25}O_3$ on the basis of a rigid-band model. One can see from Fig. 6 that for an $\langle\omega\rangle=250$ K which gives a $\lambda=0.55$ for the alloy we obtain $T_c=3.6$ K which reproduces the measured value. At the $BaSbO_3$ end of the compositional spectrum, again for $\langle\omega\rangle=250$ K we find $\lambda=1.87$ and $T_c=28.4$ K. For $BaBiO_3$ the same calculation for $\langle\omega\rangle=250$ K gives $\lambda=0.71$ for the alloy and $T_c=7.6$ K and for the pure compound $\lambda=1.53$ and $T_c=24.1$ K as it is shown by the symbol $\times$ on Fig. 6. Therefore, our results for $x=0.25$ are in agreement with the observed values of T_c.

V. CONCLUSIONS

We have calculated the electronic densities of states of $BaPb_{1-x}Sb_xO_3$ for $x=0.25$ and 1.0, using the APW method and the tight-binding CPA. Our results demonstrate a near-rigid-band behavior and a charge transfer

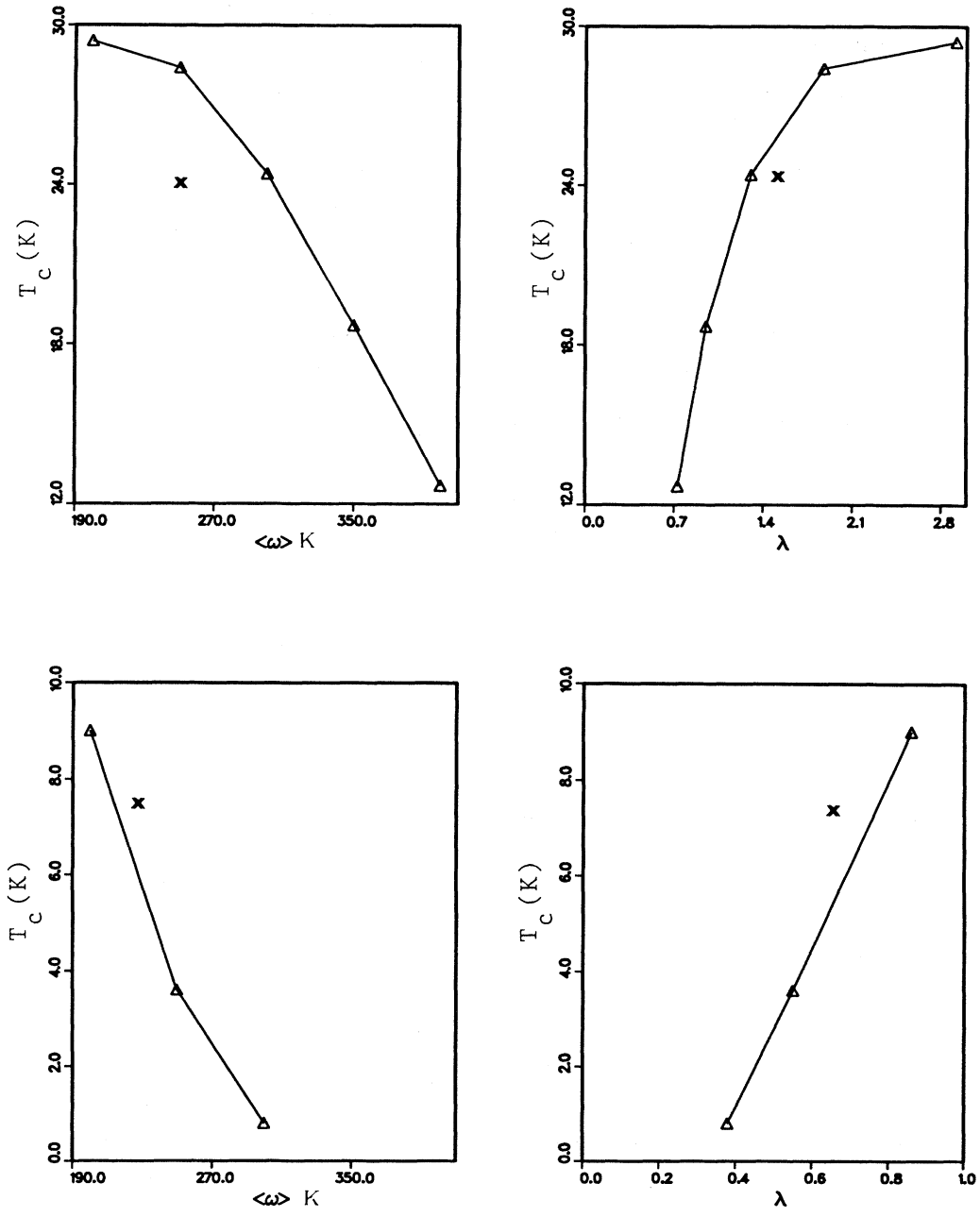

FIG. 6. Variation of T_c as a function of $\langle\omega\rangle$ and λ for pure $BaSbO_3$ (top panels) and for the rigid-band value at $x=0.25$ (bottom panels). The symbol $\times$ indicates the corresponding values for $BaBiO_3$ for $\langle\omega\rangle=250$ K.

mainly from Sb to O. We have also performed calculations of the electron-phonon interaction and of the superconducting transition temperature. Good agreement is found with the measured T_c for low Sb concentrations and a prediction is made that, for high Sb content, a value of T_c near 30 K should be expected. A comparison made with similar computations for $BaPb_{1-x}Bi_xO_3$ confirms that at $x=0.25$ the Bi-doped alloy has a higher T_c than the Sb-doped alloy, in agreement with experiment. In summary, these calculations suggest that it may be possible to further raise T_c in these systems either by increasing the Bi or Sb content or by decreasing the K content in $Ba_{1-x}K_xBiO_3$.

ACKNOWLEDGMENTS

D.A.P. would like to acknowledge partial support from the U.S. Office of Naval Research.

[1]J. C. Bednorz and K. A. Müller, Z. Phys. B **64**, 180 (1986).
[2]A. W. Sleight, J. L. Gillson, and P. E. Bierstedt, Solid State Commun. **17**, 27 (1975).
[3]B. Batlogg, Physica **126B**, 275 (1984).
[4]R. J. Cava, B. Batlogg, J. J. Krajewski, R. C. Farrow, Ja. L. W. Rupp, A. E. White, K. Short, W. F. Peck, and T. Kometani, Nature **337**, 814 (1988).
[5]C. Chaillout, A. Santoro, J. P. Remeika, A. S. Cooper, G. P. Espinosa, and M. Marezio, Solid State Commun. **65**, 1363 (1988).
[6]R. J. Cava, B. Batlogg, G. P. Espinosa, A. P. Ramirez, J. J. Krajewski, W. F. Peck, Jr., and A. S. Cooper, Nature **339**, 291 (1989).
[7]D. A. Papaconstantopoulos, A. Pasturel, J. P. Julien, and F. Cyrot-Lackmann, Phys. Rev. B **40**, 8844 (1989).
[8]L. L. Boyer, Phys. Rev. B **19**, 2824 (1979).
[9]G. Lehmann and M. Taut, Phys. Status Solidi B **54**, 469 (1972).
[10]G. D. Gaspari and B. L. Gyorffy, Phys. Rev. Lett. **29**, 801 (1972).
[11]J. S. Faulkner, in *Progress in Materials Science*, edited by J. W. Christian, P. Haasen, and T. B. Massalski (Pergamon, Great Britain, 1982), Vol. 27.